Journal of Applied Mechanics Vol.8, pp.959-966 (August 2005) JSCE

Scattering Analysis of Lamb Waves in a Perpendicularly Bent Plate

直角に曲げられた板における板波の散乱解析

Arief GUNAWAN* and Sohichi HIROSE**
グナワン アリーフ・廣瀬壮一

*Member, MS, Dept. Mechanical and Environmental Informatics, Tokyo Institute of Technology. (O-okayama, Meguro-ku, Tokyo 152-8552)
**Member, Dr. Eng., Prof., Dept. Mechanical and Environmental Informatics, Tokyo Institute of Technology. (O-okayama, Meguro-ku, Tokyo 152-8552)

Scattering analysis of Lamb waves in perpendicularly bent plates with and without a crack is presented. Single cracks on the inner or outer surface of a bent part with various lengths are considered. The scattering behaviors of Lamb waves in the bent plate with or without a crack are discussed in order to investigate the potential of Lamb wave ultrasonic method for characterizing cracks in a bent part. Experimental results are also carried out to verify the numerical results.

Key Words : *Lamb waves, scattering analysis, bent plate, crack, experiment*

1. Introduction

The application of Lamb wave ultrasonic method to nondestructive detection of a defect in a thin plate has attracted great attention recently. The Lamb wave method has an advantage that it can scan the area between the transmitting and receiving transducers. Therefore, the Lamb wave method can give a fast inspection of defects in a plate. The ability of Lamb waves to detect defects in a plate has been reported in several papers. Alleyne and Cawley[1], Lowe and Diligent[2], Koshiba *et al.*[3], Al-Nassar *et al.*[4], and Cho *et al.*[5] presented the scattering analysis of Lamb waves by notches on the surface of a plate. Rokhlin[6], Crane *et al.*[7], and Castaings *et al.*[8] performed the scattering analysis by cracks inside a plate. Lowe *et al.*[9] investigated the transmission of Lamb waves across adhesively bonded lap joints of two plates. In this paper, the scattering analysis of Lamb waves in perpendicularly bent plates with and without a crack is presented by using the mode-exciting method[10]. The single cracks on the inner or outer surface of the bent part with various lengths are considered. The scattering behaviors of Lamb waves in the bent plates with and without a crack are discussed in order to investigate the ability of Lamb wave ultrasonic method in characterizing cracks in a bent part. Experimental study is also performed to verify the numerical results.

A statement of the scattering problem of Lamb waves are presented in Section 2. Numerical results and discussion on the scattering coefficient are shown in Section 3. Section 4 presents the experimental study, which is followed by the conclusion in Section 5.

2. Scattering problem of Lamb waves

In this paper, we consider a perpendicularly bent infinite plate with curvature radius r of the center plane as shown in Fig. 1. The plate is assumed to be homogeneous, isotropic and linearly elastic.

The dispersive relations of Lamb wave modes propagating in a flat plate with free surfaces are described as[11]

$$\frac{\tan(qh)}{\tan(ph)} + \frac{4k^2pq}{(q^2-k^2)^2} = 0, \quad \text{and} \tag{1}$$

$$\frac{\tan(qh)}{\tan(ph)} + \frac{(q^2-k^2)^2}{4k^2pq} = 0, \tag{2}$$

for symmetric modes and antisymmetric modes, respectively, where k and ω denote the wavenumber and the circular frequency, respectively, and h is the half of the thickness of the plate. In Eq. (1),

$$p^2 = \frac{\omega^2}{c_L^2} - k^2, \qquad q^2 = \frac{\omega^2}{c_T^2} - k^2, \tag{3}$$

where c_L and c_T are the velocities of the longitudinal and transverse waves, respectively. Fig. 2 shows the dispersion curves for the steel plate with c_L=5940 m/s and c_T=3200 m/s, which is used in our experimental study. Here S_m and A_m denote the symmetric modes

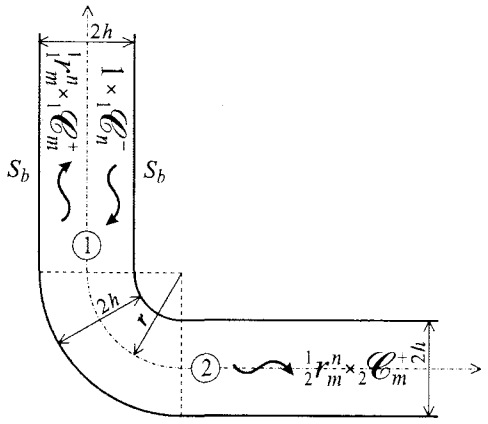

Fig. 1 Scattering problem in a perpendicularly bent infinite plate

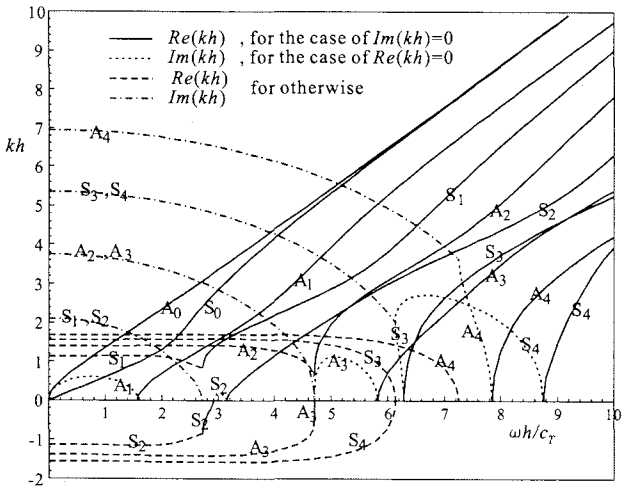

Fig. 2 Dispersion curves of Lamb wave modes in a steel plate. Solid curves and dotted curves denote the propagating waves with pure real wavenumbers and the nonpropagating waves with pure imaginary wavenumbers, respectively. Dashed curves and double dashed curves denote the real parts and the imaginary parts, respectively, of the wavenumbers of the nonpropagating waves with complex wavenumbers.

and the antisymmetric modes, respectively, of mth order (m=0, 1, 2, ...).

The scattering problem of Lamb waves in the perpendicularly bent infinite plate is defined as follows. The bent plate is composed of two flat plates ① and ② with semi-infinite lengths in which the Lamb waves propagate and the bent part which is a scatterer. Let ${}_i\mathscr{C}_n^{\pm}$ denote the propagating Lamb wave modes of nth order in the plain plate ⓘ. Here the superscripts $^-$ and $^+$ in ${}_i\mathscr{C}_n^{\pm}$ denote the incident wave propagating toward the scatterer and the scattered wave traveling away from the scatterer, respectively. It is noted here that ${}_i\mathscr{C}_n^{\pm}$ include both symmetric modes and antisymmetric modes, and are normalized in such a way that the powers of the modes with unit amplitudes are equal to unity.[10)]

Suppose that the Lamb wave ${}_1\mathscr{C}_n^-$ of the nth propagating mode in plate ① with unit amplitude is incident to the scatterer and scattered waves of all Lamb wave modes are generated in both plates ① and ② as shown in Fig. 1(a). In the far field where all scattered nonpropagating modes vanish, the scattering process can be written in the form:

$$1 \times {}_i\mathscr{C}_n^- \longrightarrow \sum_{j=1}^{2} \sum_{m=1}^{\mathcal{N}_j} {}_j^i r_m^n \times {}_j\mathscr{C}_m^+ \qquad (i=1), \quad (4)$$

where ${}_j^i r_m^n$ is the amplitude of the scattered Lamb wave ${}_j\mathscr{C}_m^+$ of the mth propagating mode in the plate ⓙ due to the incident Lamb wave ${}_i\mathscr{C}_n^-$ of the nth propagating mode in the plate ⓘ, and $\mathcal{N}_j$ is the number of propagating modes in the plate ⓙ, which depends on the frequency times the thickness of the plate as shown in Fig. 2. The arrow in Eq. (4) means the scattering process in which the incident wave ${}_i\mathscr{C}_n^-$ is transformed into the scattered waves ${}_j\mathscr{C}_m^+$ (j=1, 2; m=1, ..., $\mathcal{N}_j$). In the scattering problem of Lamb waves, ${}_j^i r_m^n$, called scattering coefficients, are the unknowns to be determined. Note that the coefficients ${}_j^i r_m^n$ are complex variables, and their square absolute values and arguments represent the powers and the phase shifts, respectively. For the cases $i = j$ and $i \neq j$, the scattering coefficients ${}_j^i r_m^n$ are called reflection coefficients and transmission coefficients, respectively. The reflection and transmission coefficients are important parameters in the Lamb wave method since they reflect the information on the crack. These coefficients are the parameters usually measured in experiments.

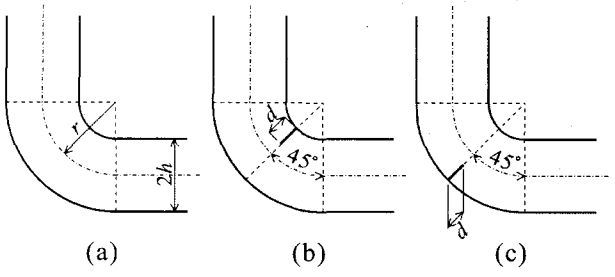

Fig. 3 Three types of perpendicularly bent plates dealt with in this study: (a) without crack, (b) with inner crack, and (c) with outer crack.

In this paper, we consider Lamb wave scattering problems in three types of perpendicularly bent plates: the bent plates without a crack, with an inner crack and with an outer crack in the bent part, which are shown in Figs. 3(a)–(c), respectively. The cracks have the length of d and are located in the middle of the bent parts and in the radial direction. The surfaces of the cracks are assumed to be traction free.

3. Numerical results

In this section, numerical results of the scattering coefficients ${}_j^i r_m^n$ are obtained for the frequencies less than the cut-off frequency of A_1 mode. A_0 and S_0 modes are the only propagating modes in this frequency range. As a model for our experimental specimen shown later, the curvature radius r/h=2.7 is adopted. The numerical method used here is the mode-exciting method. The detail description of the mode-exciting method can be found in our previously published paper[10] and will be omitted in this paper. The finite region taken for the calculation in the mode-exciting method is shown in Fig. 4. The lengths of the finite plates are taken equal to ten times of the inverse number of the smallest absolute value among the imaginary parts of the wavenumbers of nonpropagating modes. In the numerical analysis, a boundary element method with quadratic elements is applied with following discretization. The surface of the crack, the inner and outer surfaces of the bent part, and the side boundaries are divided into 10 elements, 6 elements, 10 elements, and 5 elements, respectively. The surfaces of the plates ① and ② are discretized into the elements with the length less than one-eight of the smallest wavelength of propagating mode. In numerical examples shown later, the error based on the power balance[10] is less than 1%.

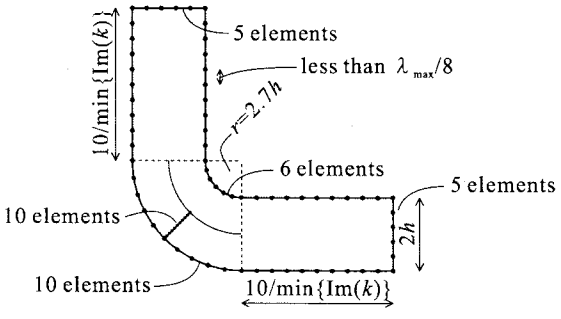

Fig. 4 BEM model in the mode-exciting method.

3.1 Bent plate without crack

The numerical results of the scattering coefficients ${}_j^i r_m^n$ for the perpendicularly bent plate without crack are shown in Figs. 5(a) and (b) for A_0 mode and S_0 mode incidences, respectively. The abscissa and ordinate represent the nondimensional frequency $\omega h/c_T$ and the absolute value of scattering coefficients $|{}_j^i r_m^n|$, respectively. This scattering problem is not symmetric problem and both A_0 and S_0 appear as scattered waves even if single mode is incident to the bent part.

It can be observed that the reflection coefficients of the same modes with the incident modes, *i.e.*, $|{}_1^1 r_{A_0}^{A_0}|$ in Fig. 5(a) and $|{}_1^1 r_{S_0}^{S_0}|$ in Fig. 5(b), increase to unity

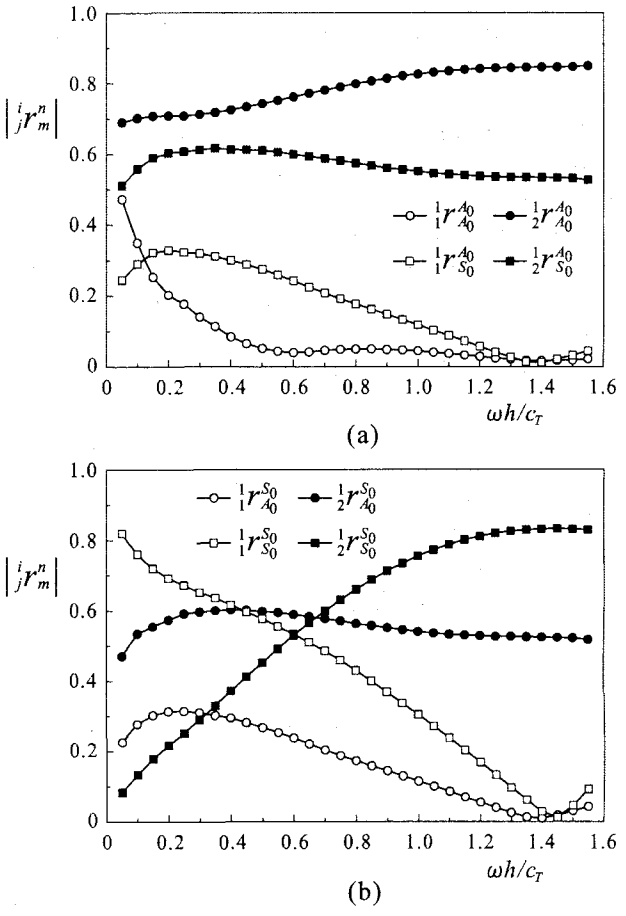

Fig. 5 Scattering coefficients for the perpendicularly bent plate without crack. (a) A_0 mode incidence and (b) S_0 mode incidence.

as the frequency becomes close to zero. This feature can be explained by considering that the wavelengths of the modes become very large compared to the thickness of the plate at the very low frequency and the wave energy hardly passes through the bent part. As the frequency increases, both reflection coefficients $|{}_1^1 r_{A_0}^{A_0}|$ and $|{}_1^1 r_{S_0}^{S_0}|$ decrease, but $|{}_1^1 r_{A_0}^{A_0}|$ decreases more rapidly than $|{}_1^1 r_{S_0}^{S_0}|$. The difference in decreasing rate between $|{}_1^1 r_{A_0}^{A_0}|$ and $|{}_1^1 r_{S_0}^{S_0}|$ can also be explained by comparing the wavelengths of both modes. The wavenumber kh of A_0 mode increases with the order $(\omega h/c_T)^{1/2}$, whereas the wavenumber of S_0 mode with the order $(\omega h/c_T)$ at relatively low frequency[11]. It means that the wavelength of A_0 mode decreases more rapidly than that of S_0 mode and the wave energy of A_0 can, therefore, pass the bent part more easily.

Owing to the power balance, the transmission coefficients of the same modes with the incident modes, $|{}_2^1 r_{A_0}^{A_0}|$ and $|{}_2^1 r_{S_0}^{S_0}|$, behaves reversely to the reflection coefficients $|{}_1^1 r_{A_0}^{A_0}|$ and $|{}_1^1 r_{S_0}^{S_0}|$. The reflection coefficients $|{}_1^1 r_{S_0}^{A_0}|$ and $|{}_1^1 r_{A_0}^{S_0}|$ and the transmission coefficients $|{}_2^1 r_{S_0}^{A_0}|$ and $|{}_2^1 r_{A_0}^{S_0}|$ decrease gradually as the frequency increases. Note that $|{}_1^1 r_{S_0}^{A_0}| = |{}_1^1 r_{A_0}^{S_0}|$ and

$|{}_2^1r_{S_0}^{A_0}| = |{}_2^1r_{A_0}^{S_0}|$ identically from the Betty's reciprocal theorem.

3.2 Bent plates with single cracks

In this subsection, the numerical results of the scattering coefficients ${}_j^ir_m^n$ for the perpendicularly bent plates with single cracks are shown in comparison with the results for the bent plate without crack. The bent plates with inner crack and outer crack shown in Figs. 3(b) and (c) with the crack lengths d/h=0.25, 0.50, 0.75, 1.00, 1.25, and 1.50 are analyzed.

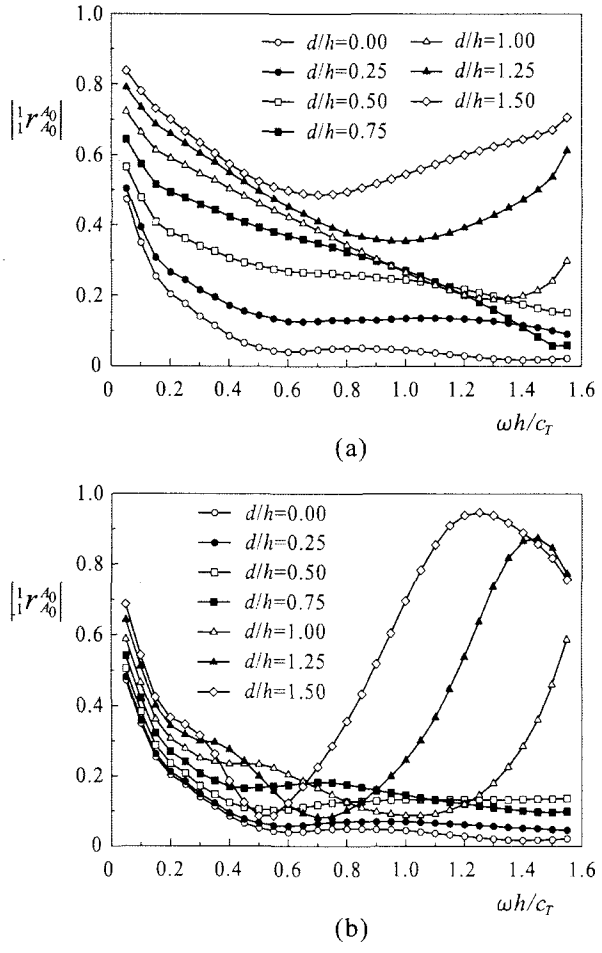

Fig. 6 Reflection coefficients $|{}_1^1r_{A_0}^{A_0}|$ as a function of frequency for the bent plates with (a) inner cracks and (b) outer cracks of various crack lengths d/h.

Figs. 6(a) and (b) show the reflection coefficients $|{}_1^1r_{A_0}^{A_0}|$ as a function of the frequency for the bent plates with inner and outer cracks having various lengths d/h, respectively. The refection coefficients for the bent plate without crack are shown in these figures by unshaded circles. As expected, for both the inner crack and the outer crack, the reflection coefficients $|{}_1^1r_{A_0}^{A_0}|$ generally increase as the crack length d/h increases. There is, however, difference between the characteristics of the increases of $|{}_1^1r_{A_0}^{A_0}|$ for the inner and outer cracks. At the relatively low frequency, $|{}_1^1r_{A_0}^{A_0}|$ for the inner crack increases more rapidly than that for the outer crack as d/h increases. At the relatively high frequency, high maximum values appear in $|{}_1^1r_{A_0}^{A_0}|$ for the outer crack at certain frequencies and the frequencies shift to the lower frequencies as d/h increases. Such maximum values do not appear in $|{}_1^1r_{A_0}^{A_0}|$ for the inner crack.

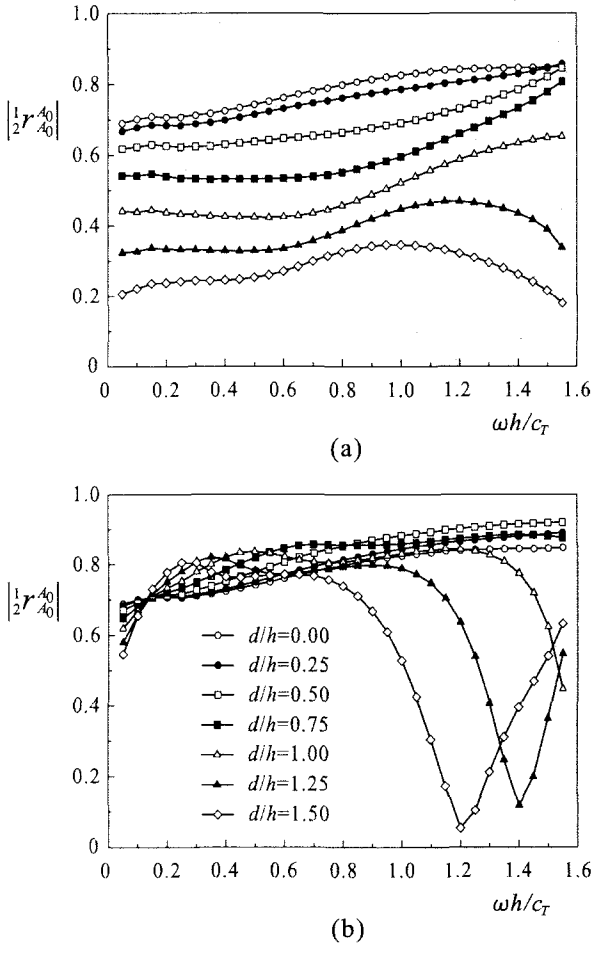

Fig. 7 Transmission coefficients $|{}_2^1r_{A_0}^{A_0}|$ as a function of frequency for the bent plates with (a) inner cracks and (b) outer cracks of various crack lengths d/h.

Figs. 7(a) and (b) show the transmission coefficients $|{}_2^1r_{A_0}^{A_0}|$ as a function of the frequency for the bent plates with inner and outer cracks, respectively. For the inner crack, $|{}_2^1r_{A_0}^{A_0}|$ decreases monotonically as the crack length d/h increases. For the outer crack, however, $|{}_2^1r_{A_0}^{A_0}|$ increases slightly for relatively small crack lengths. Also, for a large outer crack, $|{}_2^1r_{A_0}^{A_0}|$ shows a low minimum value at the frequency where the maximum value of $|{}_1^1r_{A_0}^{A_0}|$ appears in Fig. 6(b).

The reflection coefficients $|{}_1^1r_{S_0}^{S_0}|$ for the bent plates with inner and outer cracks subjected to the incident wave of S_0 mode are shown in Figs. 8(a) and (b), respectively. $|{}_1^1r_{S_0}^{S_0}|$ change very little at the very low frequency. As the frequency increases, $|{}_1^1r_{S_0}^{S_0}|$ for rela-

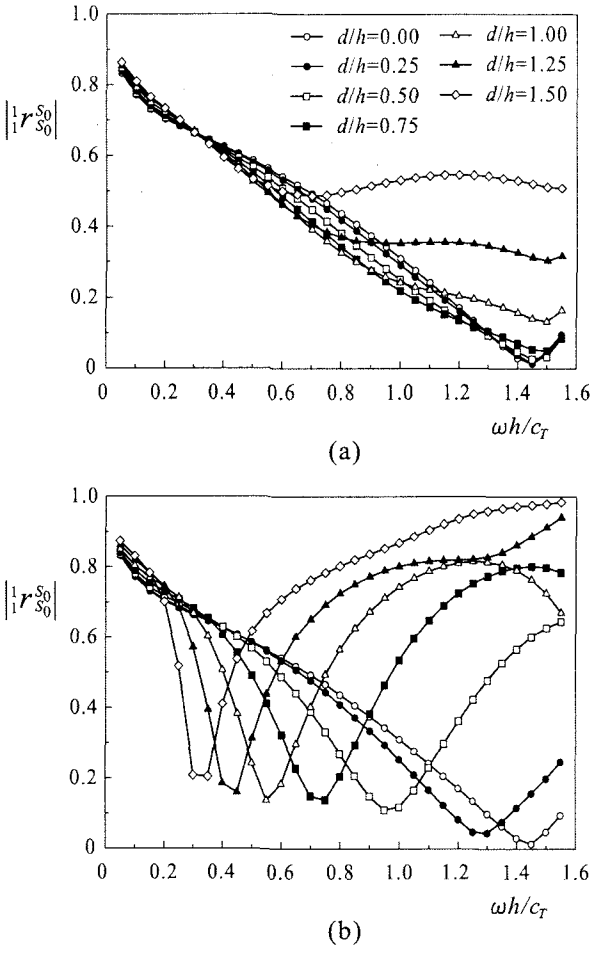

Fig. 8 Reflection coefficients $|{}_1^1r_{S_0}^{S_0}|$ as a function of frequency for the bent plates with (a) inner cracks and (b) outer cracks of various crack lengths d/h.

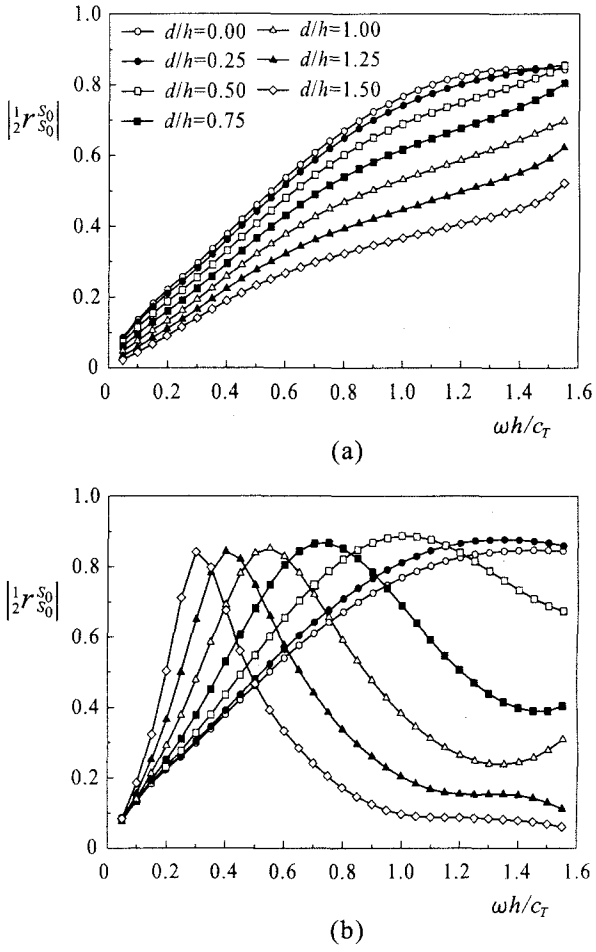

Fig. 9 Transmission coefficients $|{}_2^1r_{S_0}^{S_0}|$ as a function of frequency for the bent plates with (a) inner cracks and (b) outer cracks of various crack lengths d/h.

tively large cracks show the change. Especially for an outer crack, $|{}_1^1r_{S_0}^{S_0}|$ shows a minimum value at certain frequency and then increases in the high frequency range.

The transmission coefficients $|{}_2^1r_{S_0}^{S_0}|$ for the bent plates with inner and outer cracks are shown in Figs. 9(a) and (b), respectively. For the inner crack, $|{}_2^1r_{S_0}^{S_0}|$ increases monotonically as d/h increases. For the outer crack, $|{}_2^1r_{S_0}^{S_0}|$ shows a peak value at the frequency which depends on the crack length d/h.

Figs. 10(a) and (b) show the reflection coefficients $|{}_1^1r_{S_0}^{A_0}|=|{}_1^1r_{A_0}^{S_0}|$ for the bent plates with inner and outer cracks, respectively and Figs. 11(a) and (b) show the transmission coefficients $|{}_2^1r_{S_0}^{A_0}|=|{}_2^1r_{A_0}^{S_0}|$. The changes of $|{}_1^1r_{S_0}^{A_0}|=|{}_1^1r_{A_0}^{S_0}|$ and $|{}_2^1r_{S_0}^{A_0}|=|{}_2^1r_{A_0}^{S_0}|$ are complicated because of mode conversion.

4. Experimental study

The experimental setup is shown in Fig. 12. A pulse generator delivers an electrical signal to a transducer. The transducer has a wide frequency range with the 0.5 MHz central frequency. The transducer is set on the inclined wedge so that Lamb waves are excited by the refraction of the longitudinal wave propagating through the wedge. To obtain a wide range of inspection's frequency, a 3-cycle toneburst shown in Fig. 13(a). A laser vibrometer is used as a receiver to measure the normal velocity on the plate surface. For the measurement at multiple points, the laser vibrometer scans along a line parallel to the incident Lamb wave propagation direction. The signal detected by the laser vibrometer is sent to an oscilloscope to record the waveform with 0.1 μsec sampling time at each point of measurement. To improve the signal-to-noise ratio, we average 512 successive waveforms. The recorded signals are then sent to a computer for further signal processing.

Three specimens of the perpendicularly bent steel plates with the material properties of c_L=5940 m/s and c_T=3200 m/s are prepared in our experiment. Each specimen has the thickness of 2 mm, the width of 150 mm, the length of 250 mm for each straight part,

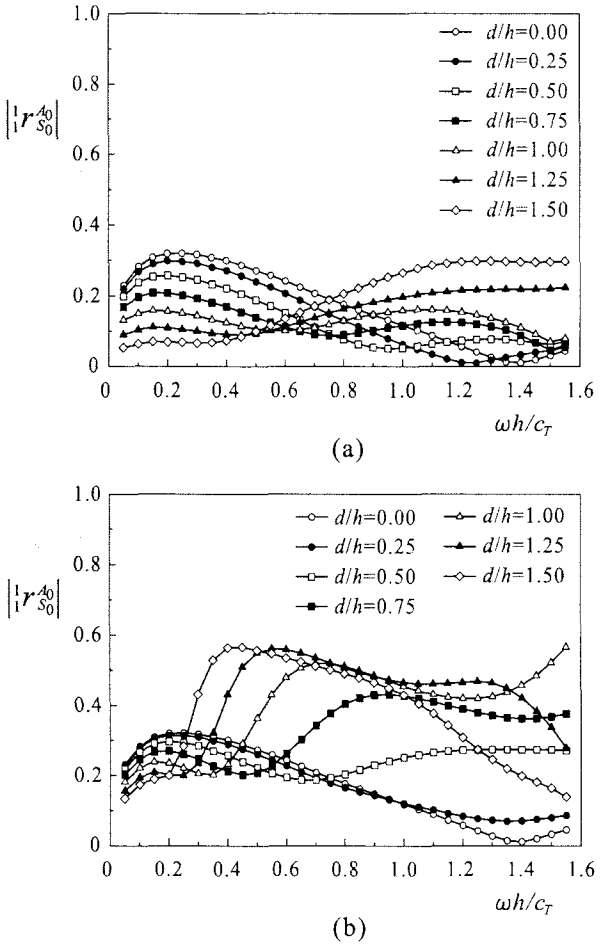

Fig. 10 Reflection coefficients $|{}_1^1r_{S_0}^{A_0}|=|{}_1^1r_{A_0}^{S_0}|$ as a function of frequency for the bent plates with (a) inner cracks and (b) outer cracks of various crack lengths d/h.

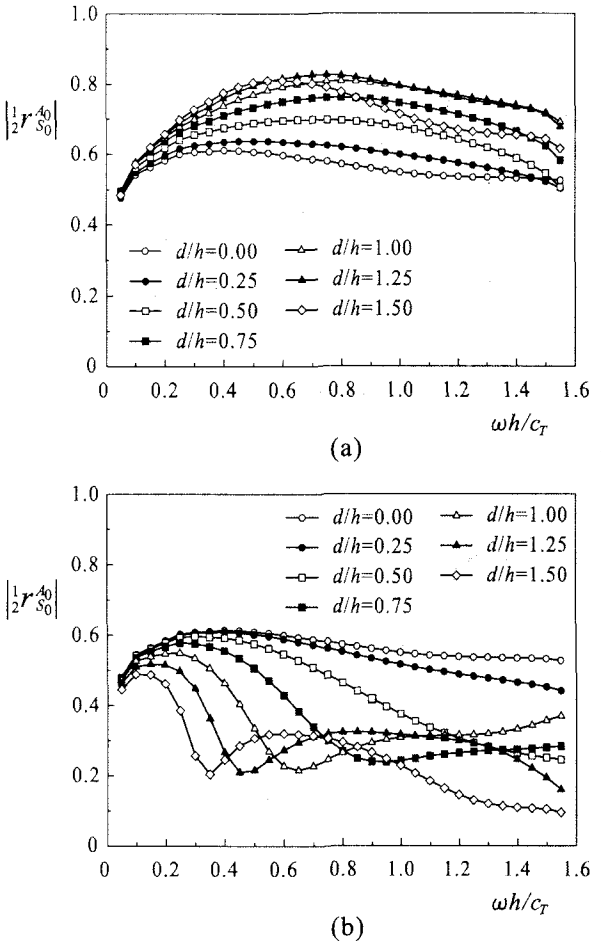

Fig. 11 Transmission coefficients $|{}_2^1r_{S_0}^{A_0}|=|{}_2^1r_{A_0}^{S_0}|$ as a function of frequency for the bent plates with (a) inner cracks and (b) outer cracks of various crack lengths d/h.

and the curvature radius r of 2.7 mm. One specimen has no defect in the bent part, whereas inner and outer cracks are processed by laser in the bent part of other two specimens shown in Fig. 3. The length and the width of each crack are 1 mm and 0.15 mm, respectively.

At a low frequency, it is known that an S_0 mode has small normal surface displacement so that it is hard to detect an S_0 mode by the laser vibrometer. In our experiment, therefore, an A_0 is measured. The incident angle of the transducer set on the wedge is chosen as 30°. The transducer with this incident angle can generate an A_0 mode as well as S_0 mode. Since the group velocities of the two modes are, however, quite different, the incident A_0 mode can be separated from the incident S_0 mode in the time domain.

In order to obtain the reflection coefficient $|{}_1^1r_{A_0}^{A_0}|$ and the transmission coefficient $|{}_2^1r_{A_0}^{A_0}|$ from experiment, three types of measurements are performed as shown in Fig. 14. Fig. 14(a) shows the measurement setup for the reflected wave from the bent part. The transducer is fixed at x=c and the signals are measured at 32 points in the range $a \leq x \leq b$ on the same side with the transducer. Here a=10 mm, b=41 mm, c=50 mm. To obtain the transmitted wave through the bent part, the transducer is also fixed at x=c but the signals are measured at 32 points in the range $a \leq z \leq b$ on the opposite side to the transducer position, as shown in Fig. 14(b). The numerical computation is carried out for 2-D problems, but the wave field in experiment has 3-D configuration. Since there is a difference in attenuation between 2-D and 3-D wave fields, the measurement shown in Fig. 14(c) is carried out as a reference to correct the amplitude decay. Note that the propagation distances of the waves for the measurements in Figs. 14(a), (b), and (c) are all the same.

The signals obtained by the measurement system shown in Figs. 14(a), (b), and (c) are Fourier transformed with respect to time and measurement position[12] to obtained the amplitudes $A_r(\omega,k)$, $A_t(\omega,k)$, and $A_i(\omega,k)$ in the frequency-wavenumber domain of the reflected, transmitted and reference waves, respectively. The reflection coefficient $|{}_1^1r_{A_0}^{A_0}|$

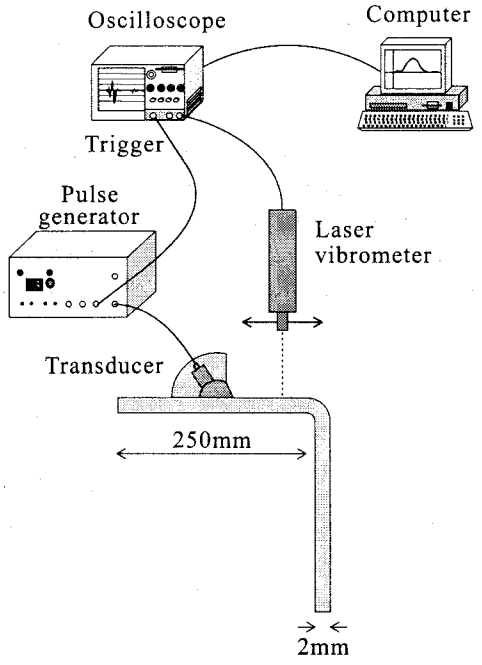

Fig. 12 Experimental setup.

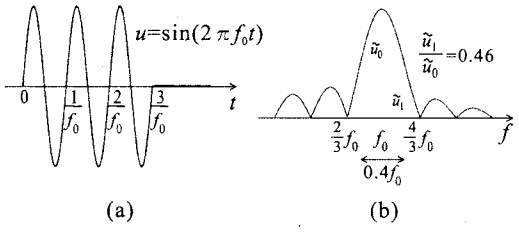

Fig. 13 (a) 3-cycle toneburst signal at the frequency f_0 and (b) its Fourier transform.

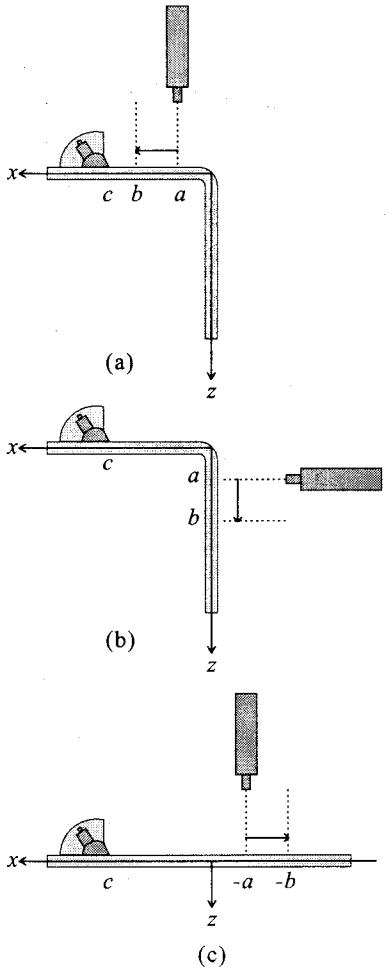

Fig. 14 Measurement setups of (a) a reflected wave and (b) a transmitted wave, and (c) a reference wave in a flat plate.

and the transmission coefficient $|{}^1_2 r^{A_0}_{A_0}|$ is then found as

$$|{}^1_1 r^{A_0}_{A_0}| = \frac{A_r(\omega, k^{A_0}(\omega))}{A_i(\omega, k^{A_0}(\omega))}, \tag{5}$$

$$|{}^1_2 r^{A_0}_{A_0}| = \frac{A_t(\omega, k^{A_0}(\omega))}{A_i(\omega, k^{A_0}(\omega))}, \tag{6}$$

where $k^{A_0}(\omega)$ is the wavenumber of the A_0 mode, which is a function of ω.

The frequencies of 3-cycle toneburst used in the experiment are f_0=0.4 MHz and f_0=0.625 MHz, or in nondimensional frequency, $\omega_0 h/c_T$=0.785 and $\omega_0 h/c_T$=1.23. The scattering coefficients in Eqs. (5) and (6) are found for the range of $0.8\omega_0 \leq \omega \leq 1.2\omega_0$. Note that the ratio of the Fourier amplitudes of the input signal at $(1 \pm 0.2)f_0$ and that at f_0 is 0.46 as shown in Fig. 13(b).

Experimental results are shown by circles in Figs. 15(a), (b), and (c) for the bent plates without crack, with the inner crack, and with the outer crack, respectively. Note that since the experiment is carried out at two main frequencies $\omega_0 h/c_T$=0.785 and $\omega_0 h/c_T$=1.23, two groups of circles appear in each figure. The numerical results are shown by solid and dashed curves. Some errors between the numerical and experimental results are observed. The errors could be attributed to manufacturing error of the bent plates and the cracks, or 3-D effects which are not considered in our 2-D analysis. The errors are particularly large at a relatively high frequency ($\omega_0 h/c_T$=1.23) because the effect of the error sources becomes more significant at a higher frequency. Though there are some errors, the reflection and transmission coefficients obtained experimentally are compatible with numerical results. Particularly, the difference between the bent plate without a crack and with cracks can be clearly seen in these figures.

5. Conclusions

The scattering analysis of Lamb waves in perpendicularly bent plates without crack and with inner and outer cracks of several lengths were carried out by using the mode-exciting method. The scattering

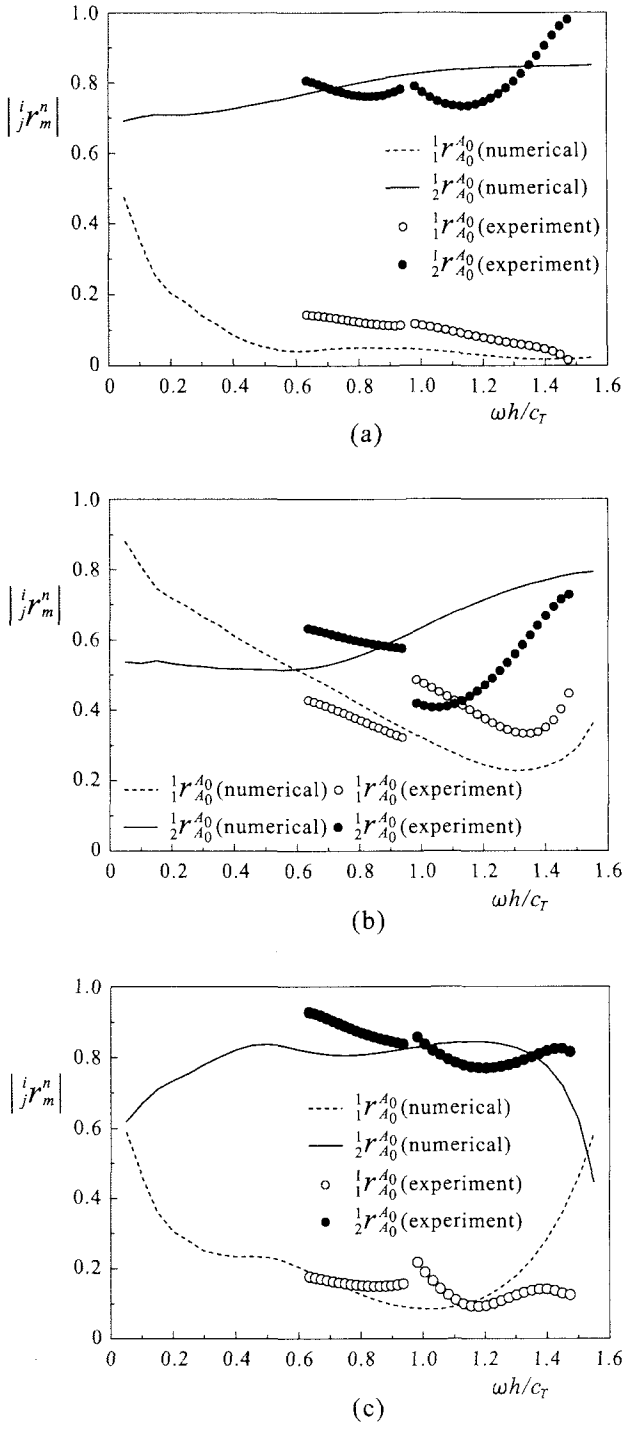

Fig. 15 Experimental results in the comparison with the numerical results for the bent plate (a) without a crack, (b) with the inner crack, and (c) with the outer crack.

coefficients as a function of frequency were calculated for various cracks and were discussed in detail. The differences among the scattering coefficients of various cracks showed the possibility for the characterization of the crack. The experiment was also performed to verify the numerical results.

The models of bent plates analyzed in this study are restricted to particular ones which conform the specimens used in the experimental study. In general, the numerical results depend largely on the model adopted in the analysis. To obtain an integrated understanding of the scattering behaviors of Lamb waves in bent plates with cracks, in the future, the analysis has to be carried out for various models, such as the plates with different curvature radii of the bent parts and different crack locations and orientations.

REFERENCES

1) D. N. Alleyne and P. Cawley: The interaction of Lamb Waves with Defect, *IEEE Trans. Ultrason. Ferroelect. Freq. Contr.* 39, 3, pp. 381–397, 1992.
2) M. J. S. Lowe and O. Diligent: Low-frequency reflection characteristics of the S_0 Lamb wave from a rectangular notch in a plate, *J. Acoust. Soc. Am.* 111(1), pp. 64–74, 2002.
3) M. Koshiba, S. Karakida, and M. Suzuki: Finite-element analysis of Lamb waves scattering in an elastic plate waveguide, *IEEE Trans. Son. and Ultrasonics* 31, pp. 18–25, 1984.
4) Y. N. Al-Nassar, S. K. Datta, and A. H. Shah: Scattering of Lamb waves by a normal rectangular strip weldment, *Ultrasonics* 29, pp. 125–132, 1991.
5) Y. H. Cho and J. L. Rose: Lamb wave scattering analysis for reflector characterization, *IEEE Trans. Ultrason. Ferroelect. Freq. Contr.* 44, pp. 44–52, 1997.
6) S. I. Rokhlin: Diffraction of Lamb waves by a finite crack in an elastic layer, *J. Acoust. Soc. Am.* 67(4), pp. 1157–1165, 1980.
7) L. J. Crane, M. D. Gilchrist, and J. J. H. Miller: Analysis of Rayleigh-Lamb wave scattering by a crack in an elastic plate, *Computational Mech.* 19, pp. 533–537, 1997.
8) M. Castaings, E. L. Clezio, and B. Hosten: Modal decomposition method for modeling the interaction of Lamb waves with cracks *J. Acoust. Soc. Am.* 112(6), pp. 2567–2582, 2002.
9) M. J. S. Lowe, R. E. Challis, and C. W. Chan: The transmission of Lamb waves across adhesively bonded lap joints, *J. Acoust. Soc. Am.* 107(3), pp. 1333–1343, 2000.
10) A. Gunawan and S. Hirose: Mode-exciting method for Lamb wave-scattering analysis, *J. Acoust. Soc. Am.* 115, pp. 996–1005, 2004.
11) J. D. Achenbach: *Wave Propagation in Elastic Solids*, North-Holland, Amsterdam, 1973.
12) D. Alleyne and P. Cawley: A two-dimensional Fourier transform method for the measurement of propagating multimode-signals, *J. Acoust. Soc. Am.* 89(3), pp. 1159–1168, 1991.

(Received April 15, 2005)